Polarity Protein AF6 Controls Hepatic Glucose Homeostasis and Insulin Sensitivity by Modulating IRS1/AKT Insulin Pathway in an SHP2-Dependent Manner

Cheng Dai, Xinyu Wang, Yanjun Wu, Yi Xu, Shu Zhuo, Meiyan Qi, Weiwei Ji, and Lixing Zhan

Diabetes 2019;68:1577–1590 | https://doi.org/10.2337/db18-0695

Insulin resistance is a major contributing factor in the development of metabolic disease. Although numerous functions of the polarity protein AF6 (afadin and MLLT4) have been identified, a direct effect on insulin sensitivity has not been previously described. We show that AF6 is elevated in the liver tissues of dietary and genetic mouse models of diabetes. We generated liver-specific AF6 knockout mice and show that these animals exhibit enhanced insulin sensitivity and liver glycogen storage, whereas overexpression of AF6 in wild-type mice by adenovirus-expressing AF6 led to the opposite phenotype. Similar observations were obtained from in vitro studies. In addition, we discovered that AF6 directly regulates IRS1/AKT kinase-mediated insulin signaling through its interaction with Src homology 2 domain-containing phosphatase 2 (SHP2) and its regulation of SHP2's tyrosine phosphatase activity. Finally, we show that knockdown of hepatic AF6 ameliorates hyperglycemia and insulin resistance in high-fat diet–fed or *db/db* diabetic mice. These results demonstrate a novel function for hepatic AF6 in the regulation of insulin sensitivity, providing important insights about the metabolic role of AF6.

Obesity-associated insulin resistance is a hallmark of type 2 diabetes and plays a central role in the metabolic syndrome (1–3). In the state of insulin resistance, the effect of insulin is repressed; the resulting excess of hepatic glucose production contributes to hyperglycemia (4). Liver is the dominant organ in the maintenance of glucose homeostasis, a function that occurs primarily through multiple insulin-mediated events (5). Thus, identifying genes and pathways that govern hepatic glucose metabolism is critical for the development of effective therapies for type 2 diabetes.

Recently, studies have implied a novel role of polarity proteins in the regulation of cell metabolism. For example, tissue-specific deletions of liver kinase B1 (LKB1) in liver (6), skeletal muscle (7,8) and pancreas (9,10) have revealed that LKB1 functions to control glucose homeostasis and energy metabolism in various tissues. Moreover, the polarity kinases PAR-1a and PAR-1b have also been reported to regulate glucose tolerance and adiposity in vivo (11,12). Linkage between cell polarity and regulation of metabolism is likely important in normal cell development and metabolic disease, which needs further investigation. AF6 (also known as afadin and MLLT4) is a multidomain F-actin–binding protein that is expressed in almost all epithelial tissues (13). AF6 plays an essential role in cell-cell junction organization and development (13–15). As a polarity protein, AF6 usually interacts with various proteins (receptor tyrosine kinases, cell adhesion molecules, regulatory and signaling molecules) to exert its effect (16–19). Notably, AF6 has been reported to attenuate phosphorylation of AKT, the major component of insulin signaling in epithelial homeostasis and oncogenesis (20–22). Because of its potent connection to PI3K/AKT signaling, we began to consider the possibility that the polarity protein AF6 might function as a regulator of glucose metabolism and insulin sensitivity.

In the current study, we show that AF6 is elevated in the livers of high-fat diet (HFD)–induced diabetic mice and *db/db* mice. We performed in vivo and in vitro experiments to test our hypothesis regarding the function of AF6 in glucose homeostasis and insulin sensitivity. Using gain-of-function and loss-of-function approaches, we demonstrate

CAS Key Laboratory of Nutrition, Metabolism and Food Safety, Shanghai Institute of Nutrition and Health, Shanghai Institutes for Biological Sciences, University of Chinese Academy of Sciences, Chinese Academy of Sciences, Shanghai, China

Corresponding author: Lixing Zhan, lxzhan@sibs.ac.cn

Received 28 June 2018 and accepted 21 May 2019

This article contains Supplementary Data online at http://diabetes.diabetesjournals.org/lookup/suppl/doi:10.2337/db18-0695/-/DC1.

that AF6 exacerbates insulin resistance through its interaction with Src homology 2 domain-containing phosphatase 2 (SHP2) and its regulation of SHP's tyrosine phosphatase activity. Furthermore, we assessed the effect of AF6 knockdown on glucose metabolism in two diabetic mouse models. Our findings reveal a novel role for the polarity protein AF6 in the regulation of insulin sensitivity, suggesting AF6 as a potential target for the treatment of diabetes.

RESEARCH DESIGN AND METHODS

Animals and Treatment

All mice were males aged 8–12 weeks, maintained on a C57BL/6J background under a 12-h light/dark cycle at 25°C, and provided free access to water and food. Wild-type (WT) and leptin receptor–mutated (*db/db*) mice were obtained from Shanghai Laboratory Animal Co. (Shanghai, China). $AF6^{flox/+}$ mice were generated by standard homologous recombination at Shanghai Biomodel Organism (Shanghai, China) and backcrossed to WT C57BL/6J mice for at least six generations. $AF6^{flox/flox}$ (AF6 fl/fl) mice were crossed with *albumin-Cre* mice to generate liver-specific AF6 knockout (AF6 LKO) offspring. Primers used for genotyping AF6 knockout (KO) are as follows: AF6-KO-p1, 5′-TGACAGGATGGCAAAC TCT-3′; AF6-KO-p2, 5′-GAGGGACCGTGTAGGAGAC-3′. Mice were fed an HFD (D12492; Research Diets) or control chow (Shanghai Laboratory Research Center, Shanghai, China) for the same period. Food intake and body weight were measured weekly. All animals were anesthetized and subjected to terminal bleeding before euthanasia. The resulting serum was stored at −80°C; tissues were collected and snap frozen in liquid nitrogen pending further analysis. All experimental procedures were approved by the institutional animal care and use committee of the Shanghai Institutes for Biological Sciences, Chinese Academy of Sciences.

Cell Culture and Treatments

The 293T cells were obtained from the American Type Culture Collection (Manassas, VA) and grown in DMEM (Thermo Fisher Scientific) containing 10% FBS (HyClone) and 1% penicillin/streptomycin (Thermo Fisher Scientific). Mouse primary hepatocytes were prepared by collagenase perfusion as described previously (23). The isolated primary hepatocytes were cultured in DMEM supplemented with 10% FBS and 1% penicillin/streptomycin precoated overnight with 20 μg/mL collagen type I (EMD Millipore). Primary hepatocytes fasted overnight were treated with various concentrations of insulin, glucose, oleic acid (OA), or palmitic acid (PA) to examine the expression of AF6.

Double-stranded small interfering RNA (siRNA) targeting mouse *SHP2* was purchased from Ribobio (Guangzhou, China). The siRNA sequences specific for mouse *SHP2* were as follows: si-SHP2-1, 5′-CCACUUUGGCUGAACUGGUU-CAGUA-3′; si-SHP2-2, 5′-GTTAGGAACGTCAAAGAAA-3′.

Generation and Administration of Recombinant Adenoviruses

The *AF6* cDNA was amplified from an AF6 overexpression vector described previously (24) and cloned into pAdeno-MCMV adenoviral backbone vector (OBiO Technology, Shanghai, China). The *SHP2* cDNA was amplified from mouse hepatic cDNA and cloned into pAdeno-MCMV adenoviral backbone vector. Plasmid constructions and PCR were performed using standard molecular biology techniques. Recombinant adenoviruses expressing AF6 (Ad-AF6), SHP2 (Ad-SHP2), and short hairpin RNA (shRNA) for mouse AF6 (Ad-shAF6) were then constructed using the AdMax system (OBiO Technology) according to the manufacturer's instructions. Purified high-titer stocks of amplified recombinant adenoviruses were diluted in PBS and administered at a dose of 1×10^7 plaque-forming units (PFU)/well in 12-well plates or injected at a dose of 1×10^9 PFU/mouse through a single injection into the tail vein. Injection of the adenoviruses above or control viruses did not affect food consumption compared with that of control-treated animals.

Blood Glucose, Serum Insulin, HOMA-Insulin Resistance Index, and Tolerance Tests

Levels of blood glucose and serum insulin were measured with a Glucometer Elite monitor or Rat Insulin ELISA Kit (EMD Millipore), respectively. The HOMA for insulin resistance (HOMA-IR) index was calculated according to the following equation: (fasting glucose levels [mmol/L] × fasting serum insulin [μU/mL]) / 22.5.

For the glucose tolerance test (GTT), mice fasted overnight for 16 h were injected intraperitoneally (i.p.) with glucose 2 g/kg body weight. For the insulin tolerance test (ITT), mice fasted for 4 h were injected with insulin 0.75 or 1 unit/kg i.p.

Measurements of Glycogen Content

Cell glycogen content was determined as previously described (25). Liver glycogen content was determined as previously described (26).

Phosphatase Assay for SHP2

Mouse primary hepatocytes infected with adenovirus for 48 h or liver tissues were lysed in lysis buffer (25 mmol/L HEPES at PH 7.4, 150 mmol/L NaCl, 2 mmol/L EDTA, 0.5% Triton X-100) and then centrifuged at 12,000*g* for 10 min at 4°C. The supernatant was incubated with the anti-SHP2 antibody for 2 h at 4°C. Protein G-Sepharose beads (GE Healthcare) were added and further incubated for 2 h at 4°C. Immunocomplexes were extensively washed twice with lysis buffer and twice with protein tyrosine phosphatase buffer (20 mmol/L HEPES at PH 7.5, 1 mmol/L EDTA, 5% glycerol, 1 mmol/L dithiothreitol). Beads then were resuspended in 50 μL of protein tyrosine phosphatase buffer supplemented with 250 μmol/L phosphopeptide (TSTEPQpYQPGENL; EMD Millipore) and incubated for 30 min at 37°C. To assess the amount of free phosphate from reactions, aliquots of supernatants were

added to 96-well plates with 100 μL of malachite green solution (EMD Millipore) and incubated for 15 min at room temperature. Absorbances were read at 620 nm with a microplate reader. The absorbance was compared with a phosphate standard curve to determine the release of phosphate in picomoles. To control the expression levels of SHP2 in the immune complex in the assays, aliquots of the immune complexes were Western blotted using the anti-SHP2 antibody.

Insulin Signaling Analysis

Mice were fasted overnight for 16 h and injected with 5 units/kg i.p. human insulin (Novo Nordisk) or PBS; 10 min after injection, mice were killed, liver samples were snap frozen in liquid nitrogen, and proteins were extracted for Western blot analysis. Mouse primary hepatocytes infected with adenovirus for 32 h were serum starved for 16 h and treated with or without 100 nmol/L insulin for 5–15 min (as indicated in the figures), and cells were then harvested for Western blot analysis.

Western Blot and Immunoprecipitation Assay

Western blot analysis and immunoprecipitation assay were performed as previously described (24). For Western blotting, target proteins were detected using an enhanced chemiluminescence kit (Pierce), quantified by National Institutes of Health Image J software, and normalized to HSP90 or the corresponding total proteins. The primary antibodies were obtained as follows: anti-AF6 antibody (BD Transduction Laboratories); anti-p-insulin receptor (IR) (Tyr1150/1151), anti-IR-β, anti-insulin receptor substrate 1 (IRS1), anti-p-AKT (Ser473), anti-p-AKT (Thr308), anti-AKT, anti-p-glycogen synthase kinase-3β (GSK3β) (Ser9), anti-GSK3β, anti-p-STAT3 (Tyr705), anti-STAT3, anti-p-extracellular signal–regulated kinase (ERK) 1/2 (Thr202/Tyr204), anti-ERK1/2, anti-SHP2, anti-glycogen synthase (GS), anti-HSP90, and anti-HA (Cell Signaling Technology); anti-p-IRS1 (Tyr612/608 [human/mouse]) and anti-phosphotyrosine (clone 4G10) (EMD Millipore); anti-glycogen phosphorylase (PYGL) and anti-glucose-6-phosphatase (G6Pase) (Abcam); anti-PEPCK and anti-IRS2 (Santa Cruz Biotechnology); and anti-FLAG (Sigma).

RNA Isolation and Real-time PCR

Total RNA was extracted from tissues or cells using TRIzol reagent (Invitrogen), according to the manufacturer's instructions. RNA was reverse transcribed with PrimeScript RT-PCR Kit (Takara Bio) to generate cDNA for real-time PCR using SYBR Premix Ex Taq (Takara Bio) in an ABI Prism 7900HT Sequence Detection System (Thermo Fisher Scientific). Transcriptional levels for mRNA were normalized to *m36B4*. The relative expression of mRNA was calculated using the $2^{-\Delta\Delta CT}$ method. Primers used for real-time PCR are shown in Supplementary Table 1.

Histological Analysis and Immunofluorescence

Liver tissues were excised and fixed with 4% paraformaldehyde for 24–36 h. For periodic acid Schiff (PAS) staining, the paraffin-embedded specimens were sectioned at 5 μm and then stained. Immunofluorescence staining was performed with anti-AF6 antibody (BD Transduction Laboratories) as described previously (24). Fluorescence was monitored by confocal laser microscopy.

Statistics

Statistical analyses were performed using GraphPad Prism 7 software. Unpaired two-tailed Student *t* test was used for comparisons between two groups. One-way or two-way ANOVA followed by Bonferroni post hoc test was used for multiple comparisons. $P < 0.05$ was considered statistically significant. Results are expressed as mean ± SEM. All results are representative of at least three independent experiments.

RESULTS

Hepatic AF6 Expression Is Upregulated in HFD-Fed and *db/db* Mice

We examined the expression of AF6 in liver tissues in two different types of diabetic mouse models: HFD-fed mice and *db/db* mice. Mice fed HFD for 8 weeks were obese and hyperglycemic (data not shown). Both mRNA and protein levels of AF6 were significantly increased in the livers of HFD-fed mice compared with control chow-fed mice (Fig. 1*A* and *B*). Similarly, hepatic AF6 levels were higher in *db/db* mice than in WT mice (Fig. 1*C* and *D*). These data suggest that hepatic expression of AF6 is significantly upregulated in dietary and genetic mouse models of diabetes.

AF6 LKO Mice Exhibit Improved Glucose Tolerance and Insulin Sensitivity

To study the potential role of AF6 in liver metabolism, we generated a liver-conditional AF6-KO mouse with *loxP* sites flanking exon 2 of *AF6* (Fig. 2*A*). AF6 LKO mice (*albumin-Cre/AF6$^{flox/flox}$*) were obtained by crossing *AF6$^{flox/flox}$* mice with mice that expressed Cre recombinase driven by the albumin promoter. Littermate *AF6$^{flox/flox}$* (AF6 fl/fl) mice were used as controls. AF6 LKO and control mice were born in accordance with Mendelian ratio. Real-time PCR, immunofluorescence, and Western blot results confirmed efficient AF6 deletion in the livers of AF6 LKO mice (Fig. 2*B* and Supplementary Fig. 1). Although body weight and food intake were comparable between AF6 LKO and control mice maintained on the standard chow diet (Supplementary Fig. 2*A* and *B*), levels of blood glucose were significantly lower in AF6 LKO mice under both fed and fasting conditions (Fig. 2*C*), with no difference in serum insulin levels (Fig. 2*D*). The HOMA-IR index was also decreased in AF6 LKO mice (Fig. 2*E*). Consistent with these changes, blood glucose levels decreased much more quickly after challenge with glucose or insulin in AF6 LKO mice than in control mice as measured by GTT and ITT, indicating improved systemic glucose tolerance and insulin sensitivity by deletion of AF6 (Fig. 2*F* and *G*).

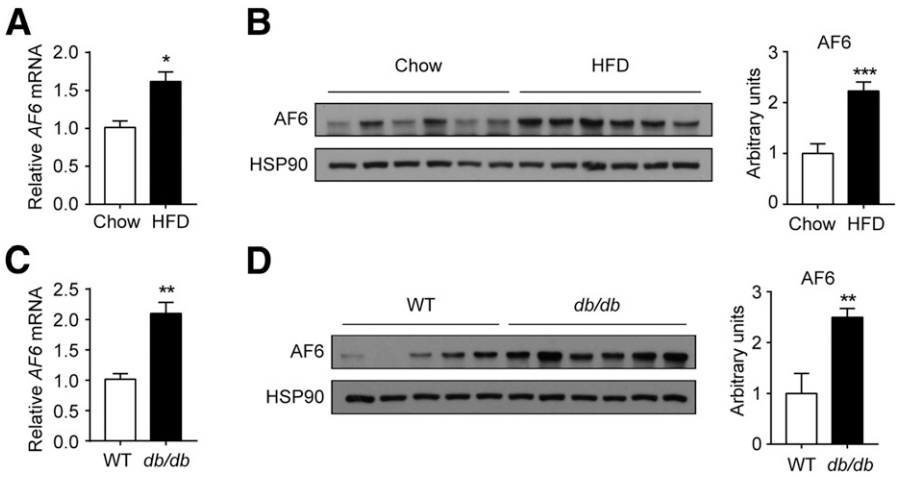

Figure 1—Hepatic AF6 expression is upregulated in HFD-fed and *db/db* diabetic mice. *A* and *B*: The mRNA (*A*) (n = 5–7 mice/group) and protein (*B*) (n = 5–7 mice/group) levels of AF6 were examined in the livers of male C57BL/6J mice fed an HFD for 8 weeks and control chow-fed mice. *C* and *D*: The mRNA (*C*) (n = 5–6 mice/group) and protein (*D*) (n = 5–6 mice/group) levels of AF6 were examined in the livers of *db/db* mice and WT mice. Densitometry analysis of AF6 protein levels relative to HSP90 is shown in *B* and *D*. Statistical analysis was performed using unpaired two-tailed Student *t* test. Data were obtained with at least three independent experiments and are mean ± SEM. $^{*}P < 0.05$, $^{**}P < 0.01$, $^{***}P < 0.001$ vs. chow-fed mice (*A* and *B*) or WT mice (*C* and *D*).

To clarify the mechanism underlying the effect of hepatic AF6 knockout on glucose homeostasis, we examined glycogen storage in the livers of AF6 LKO and control mice. PAS staining suggested that the amount of glycogen was increased in the livers of AF6 LKO mice (Fig. 2*H*). Consistent with the histology, glycogen content analysis showed that the glycogen level was approximately doubled in the AF6 LKO mice (Fig. 2*I*). These data indicate that knockout of AF6 controls glycogen metabolism in the liver. We further examined hepatic genes involved in glucose metabolism. Relevant to the glycogen alternations, AF6 deletion in the liver was found to cause a significant decrease in the mRNA level of *PYGL*, the key hepatic glycogenolysis gene (27), having an opposite effect on that of *GS*, the key glycogen synthesis gene, and glucokinase (*GK*), which catalyzes the first step of glucose metabolism (28), but scoring almost no effect on genes related to gluconeogenesis (*PEPCK*, *G6Pase*, and peroxisome proliferator–activated receptor γ coactivator-1α [*PGC-1α*]) (29) (Supplementary Fig. 3*A*). Alternations of PYGL and GS protein levels in AF6 LKO livers further confirmed the negative regulation of glycogen synthesis programmed by AF6 (Supplementary Fig. 3*C*). Given that hepatic gluconeogenic gene expression is facilitated in response to fasting, we assessed the protein levels of PEPCK and G6Pase in AF6 LKO mice during the fasting-refeeding transition but only detected a significant decrease in G6Pase expression after refeeding (Supplementary Fig. 3*E*). Additionally, we analyzed the phosphorylation of crucial participants in the insulin signaling cascade. Insulin-stimulated phosphorylation of IRS1 (Tyr608), AKT (Ser473), and GSK3β (Ser9), but not that of IR, was evidently increased in the livers of AF6 LKO mice (Fig. 2*J*). In line with increased IRS1 tyrosyl phosphorylation, there was more p85 subunit of PI3K in IRS1 immunoprecipitates from AF6 LKO livers compared with controls (Supplementary Fig. 5*A*). In addition, hepatic AF6 deficiency also resulted in increased tyrosyl phosphorylation of IRS2 (Supplementary Fig. 6*A*). These results demonstrate that hepatic knockout of AF6 could increase clearance of blood glucose most likely by promoting conversion of blood glucose into liver glycogen.

Ad-AF6 Induces Insulin Resistance in WT Mice

To further confirm the role of AF6 in insulin sensitivity, we constructed an adenovirus vector encoding the AF6 protein (Ad-AF6) and injected this construct into male C57BL/6J mice. Ad-AF6 led to increased hepatic AF6 expression compared with negative control adenovirus (Ad-NC) mice (Fig. 3*A* and *I*). Body weight and food intake did not differ significantly between the Ad-AF6 and Ad-NC animals (Supplementary Fig. 2*C* and *D*), nor did fasting blood glucose and serum insulin levels (Fig. 3*B* and *C*). However, mice infected with Ad-AF6 exhibited significantly elevated fed blood glucose and serum insulin levels as well as HOMA-IR index (Fig. 3*B–D*). Consistently, hepatic overexpression of AF6 resulted in impaired glucose tolerance and insulin sensitivity (Fig. 3*E* and *F*). Moreover, glycogen content was decreased by Ad-AF6 infection as evidenced by PAS staining and glycogen content analysis (Fig. 3*G* and *H*). In agreement with these findings, PYGL expression was enhanced and GS expression decreased in the livers of Ad-AF6 mice (Supplementary Fig. 3*B* and *D*), whereas genes related to gluconeogenesis were not affected (Supplementary Fig. 3*B* and *F*). Examination of insulin signaling showed that the insulin-induced phosphorylation of IRS1, IRS2, AKT, and GSK3β was notably decreased in the livers of Ad-AF6–infected mice (Fig. 3*I* and Supplementary

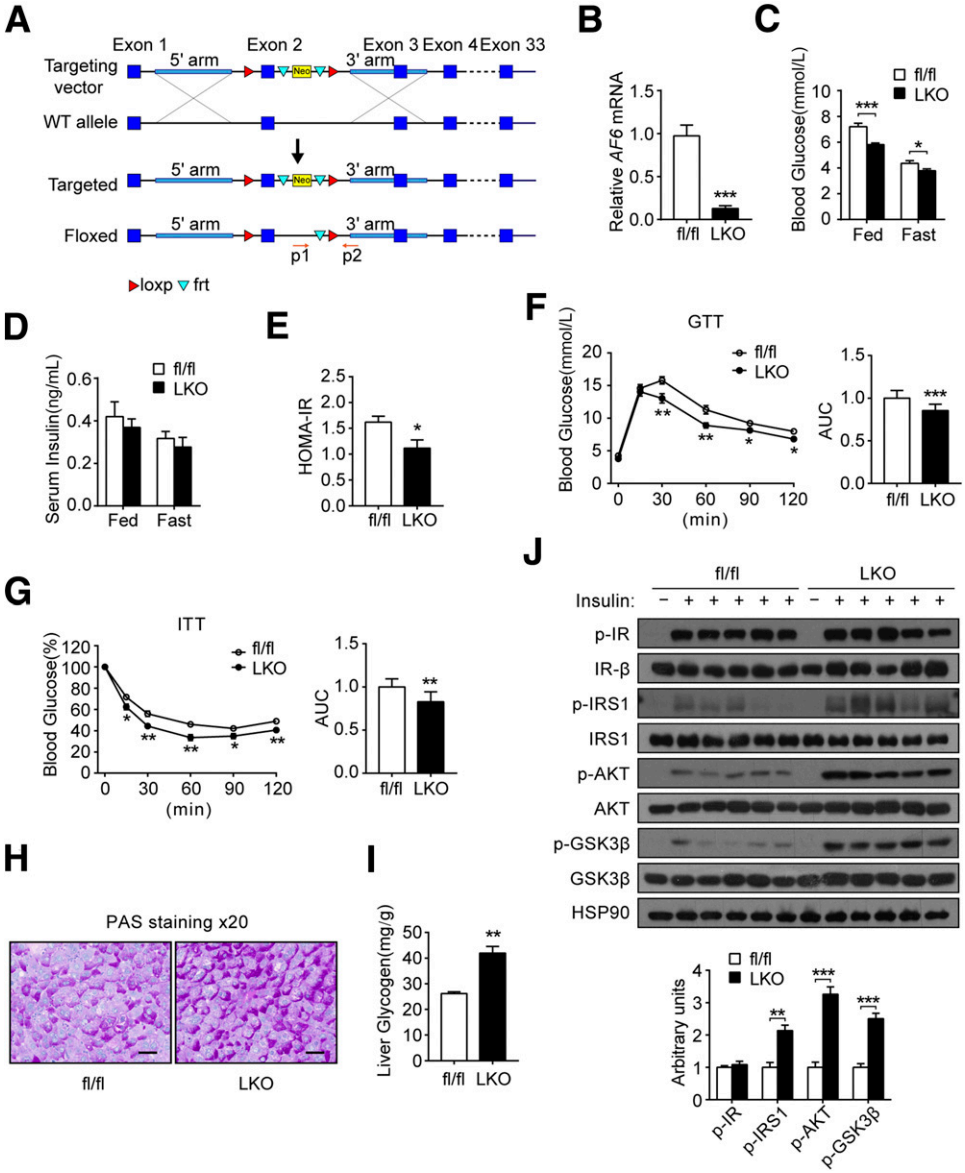

Figure 2—AF6 LKO mice exhibit improved glucose tolerance and insulin sensitivity. *A*: The targeting strategy for a conditional AF6 KO mouse. Neo, neomycin. *B–G*: Male AF6 LKO and control (AF6 fl/fl) mice were examined for hepatic AF6 mRNA levels (*B*) (n = 6–8 mice/group) followed by measurements of blood glucose (*C*) (n = 6–8 mice/group) and serum insulin (*D*) (n = 6–8 mice/group) levels under fed or fasted (18-h fast) conditions, calculation of the HOMA-IR index (*E*) (n = 6–8 mice/group), and performance of GTTs (*F*) (n = 6–8 mice/group) and ITTs (*G*) (n = 6–8 mice/group). Area under the curve (AUC) data for GTTs and ITTs also are shown. *H* and *I*: PAS staining (*H*) (n = 6–8 mice/group) and glycogen assay (*I*) (n = 6–8 mice/group) were carried out to determine the glycogen storage in the livers of AF6 LKO and control mice. Representative results of PAS staining are shown (*H*). Scale bars = 50 μm. *J*: Phosphorylated key molecules of the insulin pathway in the livers of AF6 LKO and control mice before (−) and after (+) insulin administration were determined by Western blot and quantified relative to their total proteins (n = 6–8 mice/group). Statistical analysis was performed using unpaired two-tailed Student t test (*B*, *E–G*, *I*, and *J*) or two-way ANOVA (*C* and *D*). Data were obtained with at least three independent experiments and are mean ± SEM. $^*P < 0.05$, $^{**}P < 0.01$, $^{***}P < 0.001$ vs. AF6 fl/fl mice.

Fig. 6*B*). We further examined whether re-expression of AF6 in the livers of AF6 LKO mice rescues the metabolic phenotype. As expected, restoration of AF6 expression back to a normal level totally reversed the improved effect of AF6 deletion on blood glucose, glucose tolerance, and insulin sensitivity (Supplementary Fig. 4). These results indicate that hepatic AF6 can directly induce insulin resistance in vivo.

AF6 Regulates Insulin Sensitivity In Vitro

To confirm the role of AF6 in insulin signaling, we isolated mouse primary hepatocytes from C57BL/6J mice and infected these cells in vitro with Ad-AF6 or Ad-NC. AF6 overexpression significantly impaired insulin-stimulated phosphorylation of IRS1 (Tyr608), AKT (Ser473), and GSK3β (Ser9), which suggests that Ad-AF6 induces insulin resistance (Fig. 4*A*). The opposite effects were observed

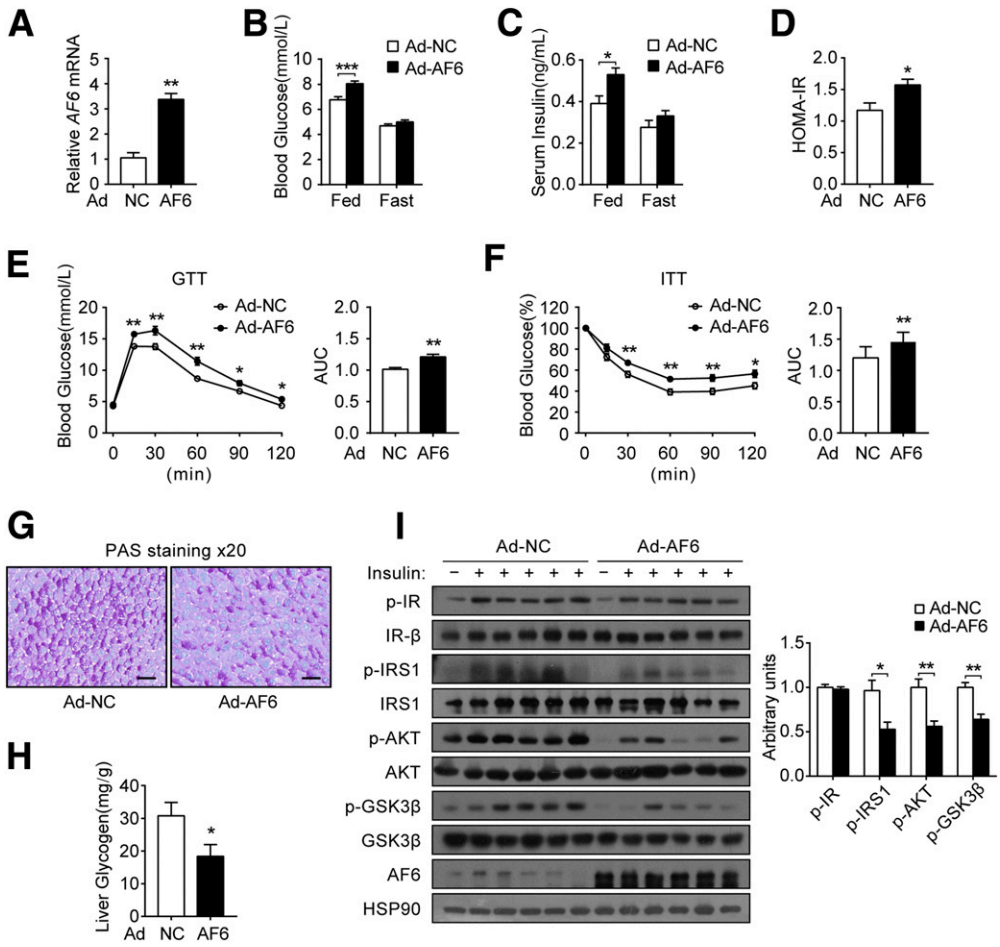

Figure 3— Ad-AF6 induces insulin resistance in WT mice. *A–F*: Male C57BL/6J WT mice infected with Ad-AF6 or Ad-NC were examined for hepatic AF6 levels (*A*) (n = 6–8 mice/group), blood glucose levels (*B*) (n = 6–8 mice/group), serum insulin levels (*C*) (n = 6–8 mice/group), GTTs (*E*) (n = 6–8 mice/group), and ITTs (*F*) (n = 6–8 mice/group); calculation of HOMA-IR index of Ad-AF6– and Ad-NC–infected mice is shown in *D*. Area under the curve (AUC) data for GTTs (*E*) and ITTs (*F*) also are shown. *G* and *H*: PAS staining (*G*) (n = 6–8 mice/group) and glycogen assay (*H*) (n = 6–8 mice/group) were carried out to determine the glycogen storage in the livers of Ad-AF6– and Ad-NC–infected mice. Representative results of PAS staining are shown (*G*). Scale bars = 50 μm. *I*: Phosphorylated key molecules of the insulin pathway in the livers of Ad-AF6– and Ad-NC–infected mice before (−) and after (+) insulin administration were determined by Western blot and quantified relative to their total proteins (n = 6–8 mice/group). Statistical analysis was performed using unpaired two-tailed Student t test (*A*, *D–F*, *H*, and *I*) or two-way ANOVA (*B* and *C*). Data were obtained with at least three independent experiments and are mean ± SEM. $^{*}P < 0.05$, $^{**}P < 0.01$, $^{***}P < 0.001$ vs. Ad-NC–infected mice.

when AF6 was knocked down by infection with Ad-shRNA specific for AF6 (Ad-shAF6) compared with control cells infected with scrambled adenovirus (Ad-scramble) (Fig. 4*C*). Insulin-stimulated phosphorylation of IR, however, was not affected by infection with either Ad-AF6 or Ad-shAF6 (Fig. 4*A* and *C*). In addition, glycogen content was significantly changed upon infection of mouse primary hepatocytes with these adenoviruses, specifically yielding decreased glycogen storage with Ad-AF6 in the presence of insulin and increased glycogen storage with Ad-shAF6 in the presence or absence of insulin (Fig. 4*B* and *D*).

AF6 Interacts With SHP2 and Increases SHP2's Phosphatase Activity

The potent function of AF6 in insulin sensitivity prompted us to explore the mechanisms underlying its effects. AF6 has been reported to regulate platelet-derived growth factor receptor activation through the protein tyrosine phosphatase SHP2 (30), and SHP2 has been shown to be a negative regulator of hepatic insulin sensitivity (31). We postulated that AF6 might regulate insulin signaling through SHP2. To test this hypothesis, we first used coimmunoprecipitation assays to assess the interaction between AF6 and SHP2. When both AF6 and SHP2 were overexpressed in 293T cells, immunoprecipitation of SHP2 could pull down AF6 (Supplementary Fig. 7*A*). Conversely, immunoprecipitation of AF6 could also pull down SHP2 (Supplementary Fig. 7*B*). Furthermore, we found that endogenous AF6 did form a complex with SHP2 in mouse primary hepatocytes (Fig. 5*A* and *B*). Interestingly, the amount of SHP2 coimmunoprecipitated with AF6 was increased in the presence of insulin in mouse primary

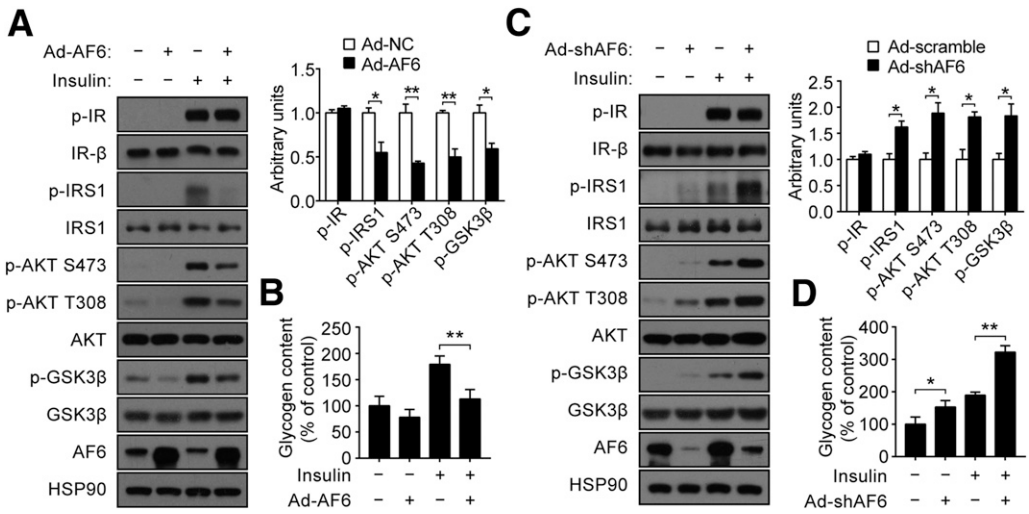

Figure 4—AF6 regulates insulin sensitivity in vitro. *A* and *C*: Mouse primary hepatocytes were infected with Ad-AF6 or Ad-NC for 48 h (*A*) or Ad-shAF6 or Ad-scramble for 48 h (*C*) and stimulated with (+) or without (−) 100 nmol/L insulin for 10 min followed by Western blot and densitometry analysis of phosphorylated key molecules of the insulin pathway. *B* and *D*: Primary hepatocytes were infected with Ad-AF6 or Ad-NC for 48 h (*B*) or Ad-shAF6 or Ad-scramble for 48 h (*D*) and then treated with (+) or without (−) 100 nmol/L insulin for another 24 h followed by measurements of glycogen content. Statistical analysis was performed using unpaired two-tailed Student *t* test (*A* and *C*) or two-way ANOVA (*B* and *D*). Data were obtained with at least three independent experiments and are mean ± SEM. $^*P < 0.05$, $^{**}P < 0.01$ vs. corresponding control.

hepatocytes (Fig. 5*C*). We speculated that insulin might stimulate AF6-mediated recruitment of SHP2 and contribute to the feedback inhibition loop. We further examined the effect of AF6 on the tyrosine phosphatase activity of SHP2. The endogenous SHP2 was immunoprecipitated from mouse primary hepatocytes infected with Ad-AF6 or Ad-NC. Next, the tyrosine phosphatase activity of SHP2 was assessed using a small phosphopeptide, TSTEPQ-pYQPGENL, as a model substrate. AF6 overexpression significantly increased the phosphatase activity of SHP2 (Fig. 5*D*). Consistently, the phosphatase activity was impaired when endogenous AF6 levels were reduced by Ad-shAF6 (Fig. 5*E*). In line with these in vitro results, phosphatase activity of hepatic SHP2 was enhanced in Ad-AF6–infected mice and attenuated in AF6-KO mice (Fig. 5*F* and *G*). Taken together, these data indicate that AF6 interacts with SHP2 and is sufficient for the activation of SHP2 tyrosine phosphatase activity.

AF6 Regulates Insulin Signaling Through SHP2

We then investigated whether SHP2 is involved in AF6-regulated insulin sensitivity. Mouse primary hepatocytes from C57BL/6J mice were isolated and transfected with two different siRNAs to downregulate SHP2 expression. Ad-AF6 significantly impaired insulin-stimulated phosphorylation of IRS1, AKT, and GSK3β, and this effect was rescued by knockdown of SHP2 (Fig. 6*A*). Furthermore, we isolated mouse primary hepatocytes from AF6 fl/fl mice and infected these cells with the combination of Ad-cre (or the control Ad-NC) and Ad-SHP2 (or the control Ad-null). As predicted, overexpression of SHP2 significantly blocked the increase in insulin-stimulated phosphorylation of IRS1, AKT, and GSK3β seen upon deletion of AF6 (Fig. 6*B*). However, SHP2 overexpression did not have an apparent effect on insulin-stimulated phosphorylation of IR in cells subjected to any of these treatments. To confirm this epistasis in vivo, we injected AF6 LKO or AF6 fl/fl mice with Ad-SHP2 and examined the effects on AF6 deficiency–improved insulin sensitivity. As we supposed, infection with Ad-SHP2 significantly elevated blood glucose and serum insulin levels in AF6 LKO mice (Fig. 6*C* and *D*). Overexpression of SHP2 also counteracted the changes of HOMA-IR index observed in AF6 LKO mice (Fig. 6*E*) as well as the improved glucose tolerance and insulin sensitivity seen with AF6 deletion (Fig. 6*F* and *G*). We next analyzed insulin signaling in the livers of these mice. Notably, SHP2 overexpression abrogated the effect of AF6 deletion on insulin-stimulated phosphorylation of IRS1, AKT, and GSK3β as well as IRS1-p85 interaction (Fig. 6*H* and Supplementary Fig. 5*B*). Considered together, these experiments clearly demonstrate that overexpression of SHP2 is able to restore insulin signaling in hepatocytes with AF6 deficiency and block the enhanced insulin sensitivity in AF6 LKO mice.

Given the ability of AF6 to affect endogenous SHP2 activity, we were interested in investigating whether overexpression of AF6 could enhance the inhibitory effect of Ad-SHP2 on glucose tolerance and insulin sensitivity. Five times less Ad-SHP2 (2×10^8 PFU/mouse) was used for in vivo experiments. SHP2 expression levels were moderately elevated in the livers of mice after Ad-SHP2 infection. A moderate amount of Ad-SHP2 had no obvious effect on levels of blood glucose, glucose tolerance, and insulin sensitivity as well as on the activation of IRS1/AKT

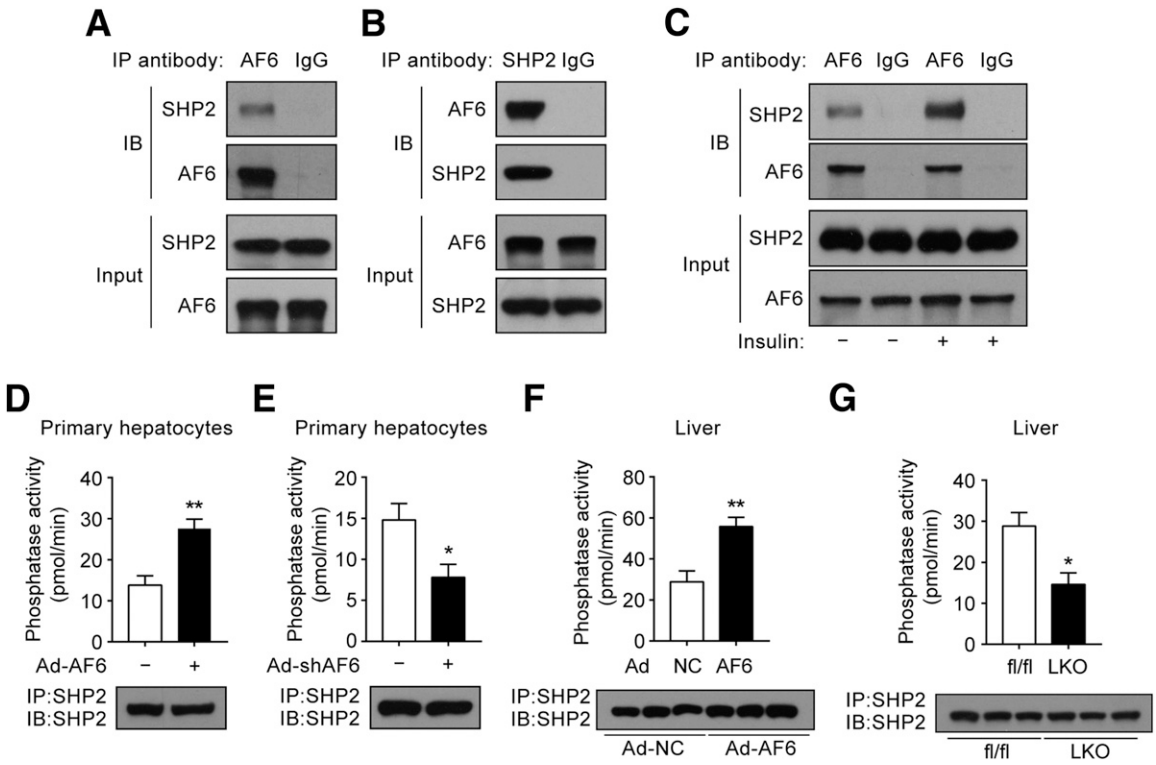

Figure 5—AF6 interacts with SHP2 and increases SHP2's phosphatase activity. *A* and *B*: Endogenous AF6 bound to endogenous SHP2 in mouse primary hepatocytes. Cell lysates from primary hepatocytes were immunoprecipitated with control mouse IgG or anti-AF6 monoclonal antibody (mAb) (*A*) or anti-SHP2 mAb (*B*) and immunoblotted as indicated. *C*: Cell lysates from primary hepatocytes stimulated with (+) or without (−) 100 nmol/L insulin for 15 min were immunoprecipitated with control mouse IgG or anti-AF6 mAb and immunoblotted as indicated. *D* and *E*: Mouse primary hepatocytes were infected with Ad-AF6 or Ad-NC for 48 h (*D*) or Ad-shAF6 or Ad-scramble for 48 h (*E*) and then subjected to the phosphatase assay for SHP2. SHP2 was immunoprecipitated from the cell lysates with the anti-SHP2 mAb. Aliquots of the immunoprecipitates were subjected to Western blot using the anti-SHP2 mAb (bottom panels). *F* and *G*: Liver tissues of C57BL/6J WT mice infected with Ad-AF6 or Ad-NC (*F*) (n = 6–8 mice/group) or AF6 LKO or control (AF6 fl/fl) mice (*G*) (n = 6–8 mice/group) were subjected to the phosphatase assay for SHP2. SHP2 was immunoprecipitated from the liver lysates with the anti-SHP2 mAb. Aliquots of the immunoprecipitates were subjected to Western blot using the anti-SHP2 mAb. Statistical analysis was performed using unpaired two-tailed Student t test. Data were obtained with at least three independent experiments and are mean ± SEM. $^*P < 0.05$, $^{**}P < 0.01$ vs. Ad-NC–infected hepatocytes (*D*), Ad-scramble–infected hepatocytes (*E*), Ad-NC–infected mice (*F*), or AF6 fl/fl mice (*G*). IB, immunoblot; IP, immunoprecipitation.

signaling; however, additional injection of Ad-AF6 significantly impaired these phenotypes (Supplementary Fig. 8). On the basis of these findings, we propose that the action of AF6 on glucose metabolism and hepatic insulin signaling is mediated through its regulation of SHP2's tyrosine phosphatase activity.

Knockdown of AF6 Ameliorates Hyperglycemia and Insulin Resistance in Diabetic Mice

The observations that AF6 depletion promotes liver glycogen storage and improves insulin sensitivity led us to hypothesize that knockdown of hepatic AF6 under diabetic conditions may be helpful for reducing blood glucose level. To address this hypothesis, we first fed AF6 LKO and control mice an HFD for an interval of 2 months, starting from the age of 8 weeks. Real-time PCR and Western blot results demonstrated almost completely abolished expression of AF6 in HFD-fed AF6 LKO mice compared with that from control mice (Supplementary Figs. 9*A* and 11*A*). These HFD-fed AF6 LKO mice exhibited significantly decreased levels of fed and fasting blood glucose and fed serum insulin, as well as a deceased HOMA-IR index, compared with HFD-fed control mice (Fig. 7*A*–*C*). Importantly, the glucose tolerance and clearance of HFD-fed mice were markedly improved by deletion of AF6 (Fig. 7*D* and *E*). In addition, AF6 LKO resulted in enhanced hepatic insulin sensitivity as evidenced by the significantly increased levels of phosphorylated IRS1, AKT, and GSK3β in the LKO mice (Supplementary Fig. 11*A*). Taken together, these results demonstrate that AF6 deficiency could alleviate hyperglycemia and insulin resistance in HFD-induced diabetic mice.

To further validate the functional role of AF6 in insulin resistant conditions, we injected *db/db* mice with Ad-shAF6 or Ad-scramble to examine whether decreased AF6 expression could reverse insulin resistance in these mice. As shown in Supplementary Figs. 9*B* and 11*B*, Ad-shAF6 infection caused efficient knockdown of endogenous AF6 in the liver. As expected, infection of *db/db* mice with Ad-shAF6 yielded significant decreases in the levels of

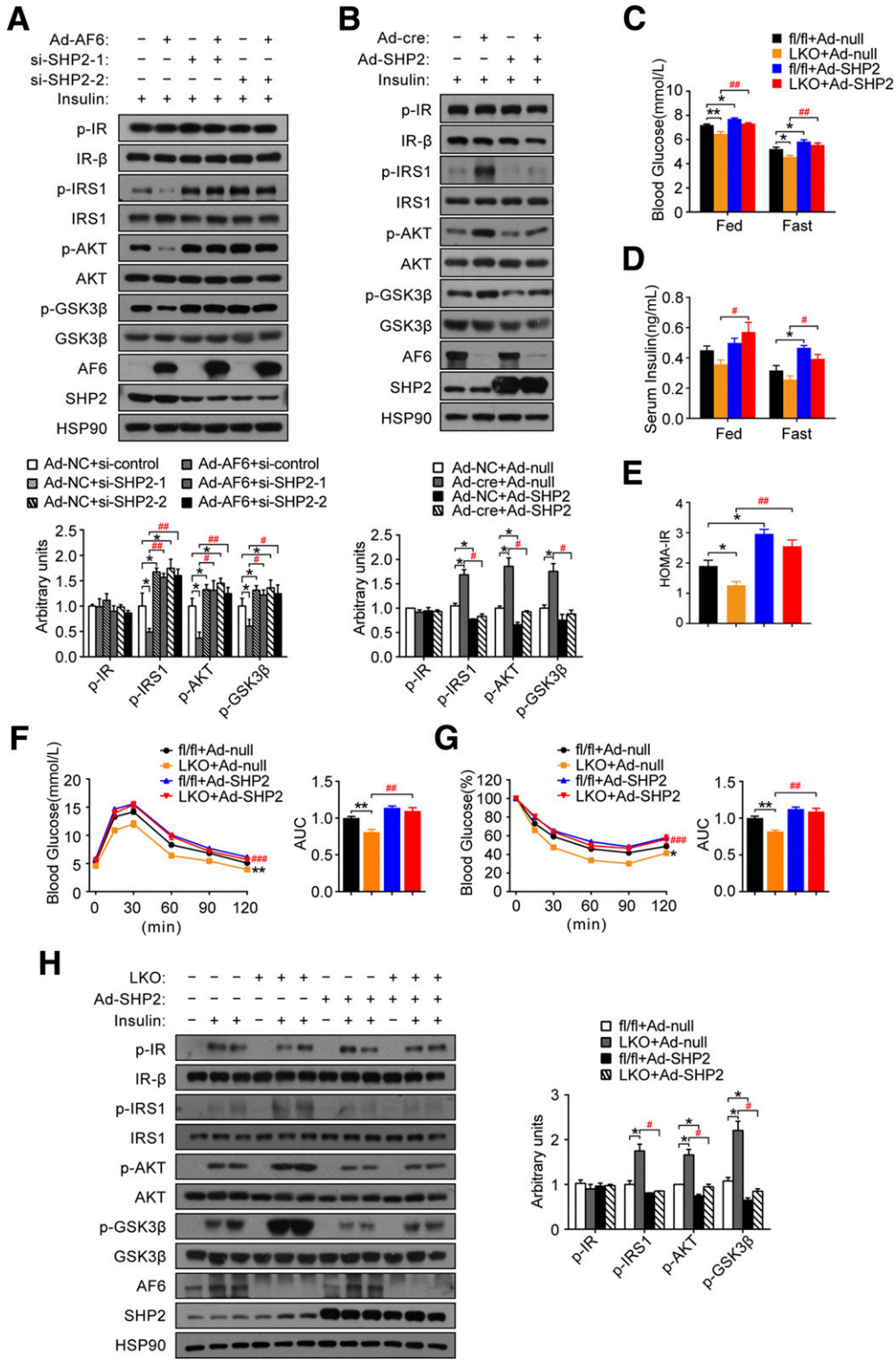

Figure 6— AF6 regulates insulin signaling through SHP2. *A*: Mouse primary hepatocytes were transfected with two different SHP2 siRNAs or control reagent (si-control) for 24 h before being infected with Ad-AF6 or Ad-NC for 48 h and then stimulated with 100 nmol/L insulin for 10 min followed by Western blot and densitometry analysis of phosphorylated key molecules of the insulin pathway. $^{*}P < 0.05$ vs. Ad-NC + si-control; $\#P < 0.05$, $\#\#P < 0.01$ vs. Ad-AF6 + si-control. *B*: Mouse primary hepatocytes from AF6 fl/fl mice were infected with Ad-SHP2 or Ad-null for 24 h and infected with Ad-cre or Ad-NC for 48 h and then stimulated with 100 nmol/L for 10 min followed by Western blot and densitometry analysis of phosphorylated key molecules of the insulin pathway. $^{*}P < 0.05$ vs. Ad-NC + Ad-null; $\#P < 0.05$ vs. Ad-cre + Ad-null. *C–G*: Male AF6 LKO and AF6 fl/fl mice were injected with Ad-SHP2 or Ad-null followed by examination of blood glucose levels (*C*) (n = 6–8 mice/group), serum insulin levels (*D*) (n = 6–8 mice/group), GTTs (*F*) (n = 6–8 mice/group), and ITTs (*G*) (n = 6–8 mice/group); calculation of the HOMA-IR index is shown in *E*. Area under the curve (AUC) data for GTTs (*F*) and ITTs (*G*) also are shown. $^{*}P < 0.05$, $^{**}P < 0.01$; $\#P < 0.05$, $\#\#P < 0.01$, $\#\#\#P < 0.001$. *H*: Phosphorylated key molecules of insulin pathway in the livers of AF6 LKO and AF6 fl/fl mice injected with

fed and fasting blood glucose and serum insulin as well as in the HOMA-IR index (Fig. 7*F–H*). Consistent with the effect of AF6 LKO in HFD-induced diabetic mice, *db/db* mice injected with Ad-shAF6 exhibited markedly enhanced glucose tolerance, insulin sensitivity, and hepatic insulin signaling (Fig. 7*I* and *J* and Supplementary Fig. 11*B*). Knockdown of AF6 in both HFD-induced diabetic mice and *db/db* mice had no significant effect on body weight and food intake (Supplementary Fig. 10). Collectively, these results suggest that depletion of AF6 in liver ameliorates hyperglycemia and insulin resistance in diabetic mice.

AF6 Expression Level Is Influenced by Nutrition in Hepatocytes

Because hepatic AF6 was elevated in diabetic mice (Fig. 1), which have hyperinsulinemia, hyperglycemia, and high levels of plasma free fatty acids (FFAs), we examined whether various concentrations of insulin, glucose, or FFAs could regulate hepatic AF6 expression in primary hepatocytes. Our results suggest that the treatment of insulin or glucose has no effect on AF6 expression, but the treatment of OA and PA could upregulate both the mRNA and the protein levels of AF6 in a dose-dependent manner in primary hepatocytes (Fig. 8*A–D* and Supplementary Fig. 12). These results indicate that hepatic AF6 might be upregulated by FFAs in diabetes and that downregulation of hepatic AF6 may be helpful for lowering blood glucose levels.

DISCUSSION

The polarity protein AF6 is expressed in almost all tissues in both embryos and adults and in a variety of cell types, including epithelial cells, neurons, and fibroblasts (13,15,32). Recent studies have implicated AF6 as playing a role in the pathogenesis of several diseases, including Parkinson disease (33,34), cardiac hypertrophy (35), and various types of cancer (24,36,37). However, the regulatory effect of AF6 on diabetes as well as its specific functions in the liver remain largely unknown. As reported here, AF6 expression is markedly increased in liver tissues of two diabetic animal models. Liver-specific AF6-KO mice exhibited improved glucose tolerance and insulin sensitivity, whereas Ad-AF6 overexpression in mice had the opposite effect, indicating that AF6 is a negative regulator of insulin signaling in the liver. In addition, our in vitro studies showed that AF6 overexpression and knockdown impairs and improves insulin signaling, respectively, in primary hepatocytes. Mechanistically, AF6 directly interacts with SHP2 and regulates SHP2's tyrosine phosphatase activity, thereby eliciting the inactivation of downstream IRS1/AKT signaling. Finally, AF6 knockdown significantly ameliorates hyperglycemia and insulin resistance in the two diabetic mouse models. In summary, our findings highlight a critical role of hepatic AF6 in the regulation of glucose homeostasis, suggesting new opportunities for treating diabetes.

The liver plays a critical role in glucose metabolism and can store or produce glucose, depending on physiological conditions. Glycogen, which is considered the principal storage form of glucose, is found primarily in liver and skeletal muscle (29). Glycogen homeostasis involves the concerted regulation of the rate of glycogen synthesis and the rate of glycogenolysis. Defects in these two processes can be major contributors to hyperglycemia and insulin resistance, and the liver glycogen content is decreased in individuals with type 2 diabetes (38). In the current study, liver glycogen storage was significantly increased in AF6 LKO mice. We examined mRNA and protein levels of key target genes implicated in glucose metabolism and found that expression of PYGL was lower and expression of GS higher in AF6 LKO livers compared with controls. We further assessed the protein levels of gluconeogenic genes *PEPCK* and *G6Pase* in AF6 LKO mice during the fasting-refeeding transition. Our results suggest that protein expression of PEPCK was slightly suppressed by deletion of AF6 after refeeding ($P = 0.051$), and the expression of G6Pase was significantly reduced in AF6 LKO mice after refeeding. We also demonstrated in vitro effects of AF6 deficiency to increase cell glycogen content in isolated mouse primary hepatocytes. In addition to deletion of AF6, we carried out Ad-AF6 administration studies in vitro and in vivo. AF6 overexpression led to lower glycogen storage as expected. These observations revealed that AF6 is a critical regulator of glycogen metabolism and suggest that AF6 induces hyperglycemia most likely by inhibiting liver glycogen storage.

The insulin signaling pathway comprises three essential mediators: the IR and related IRS, the PI3K heterodimer, and AKT (39). Our studies showed that AF6 affects phosphorylation of IRS1 and AKT but not that of IR; therefore, we predicted that the target of AF6 likely lies downstream of IR in the insulin signaling cascade. Indeed, prior work has shown that AF6 regulates platelet-derived growth factor receptor activation through the protein tyrosine phosphatase SHP2 (30). SHP2 has been reported to regulate insulin signaling by binding to and dephosphorylating the PI3K binding sites of IRS1 (31,40,41). On the basis of these studies, we hypothesized that AF6 might regulate insulin signaling by SHP2. As we show in the present work, AF6 interacts with SHP2 and increases SHP2's phosphatase activity. It was reported that SHP2 deletion in

Ad-SHP2 or Ad-null before (−) and after (+) insulin administration were determined by Western blot and quantified relative to their total proteins (n = 6–8 mice/group). *$P < 0.05$ vs. AF6 fl/fl mice injected with Ad-null; #$P < 0.05$ vs. AF6 LKO mice injected with Ad-null. Statistical analysis was performed using one-way ANOVA (*A*, *B*, and *E*, AUC in *F–H*) or two-way ANOVA (*C* and *D*, GTT in *F*, and ITT in *G*). Data were obtained with at least three independent experiments and are mean ± SEM.

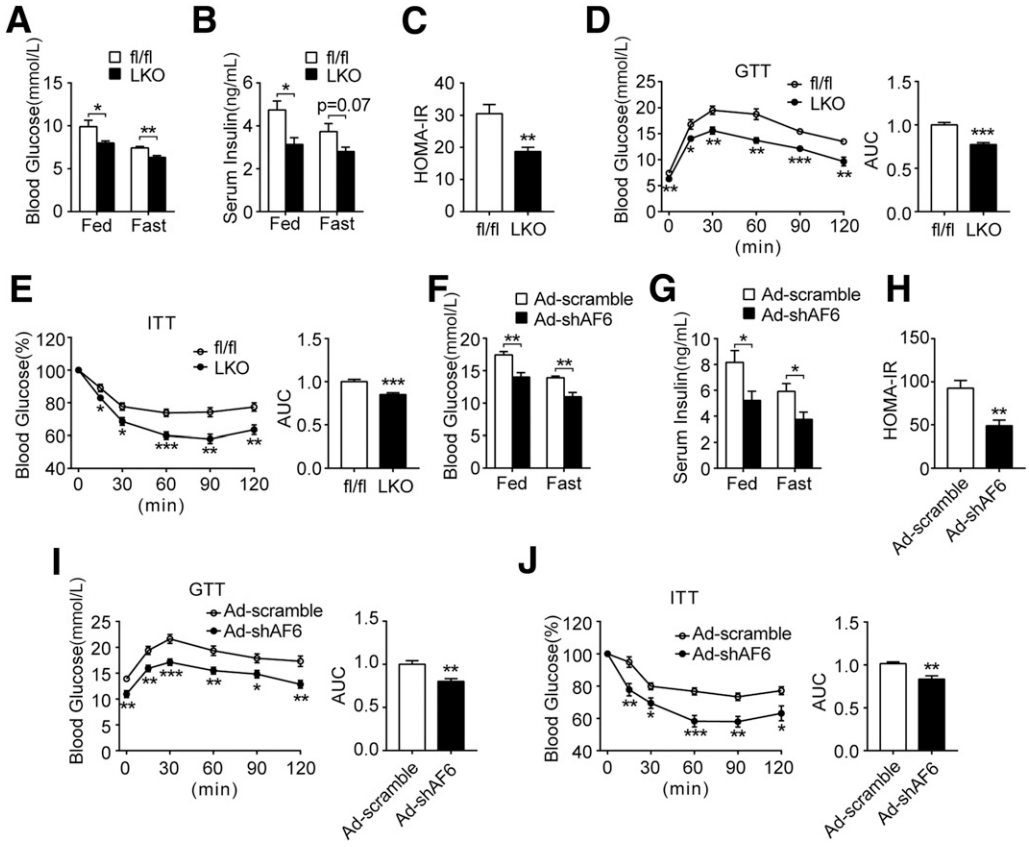

Figure 7— Knockdown of AF6 ameliorates hyperglycemia and insulin resistance in diabetic mice. *A–E*: AF6 LKO and AF6 fl/fl mice fed an HFD for 8 weeks were examined for blood glucose levels (*A*) (n = 6–8 mice/group), serum insulin levels (*B*) (n = 6–8 mice/group), HOMA-IR index (*C*) (n = 6–8 mice/group), GTTs (*D*) (n = 6–8 mice/group), and ITTs (*E*) (n = 6–8 mice/group). Area under the curve (AUC) data for GTTs (*D*) and ITTs (*E*) also are shown. *F–J*: Male C57BL/6J *db/db* mice injected with Ad-shAF6 or Ad-scramble were examined for blood glucose levels (*F*) (n = 6–8 mice/group), serum insulin levels (*G*) (n = 6–8 mice/group), HOMA-IR index (*H*) (n = 6–8 mice/group), GTTs (*I*) (n = 6–8 mice/group), and ITTs (*J*) (n = 6–8 mice/group). AUC data for GTTs (*I*) and ITTs (*J*) also are shown. Statistical analysis was performed using unpaired two-tailed Student t test (*C–E* and *H–J*) or two-way ANOVA (*A*, *B*, *F*, and G). Data were obtained with at least three independent experiments and are mean ± SEM. $^{*}P < 0.05$, $^{**}P < 0.01$, $^{***}P < 0.001$ vs. AF6 fl/fl mice (*A–E*) or Ad-scramble–infected mice (*F–J*).

hepatocytes could repress Ras/ERK signaling and drive cytokine-induced STAT3 signaling (42,43). We further designed experiments to observe the possibility that AF6 contributes to insulin sensitivity by activation of ERK1/2 or STAT3. We examined phosphorylation of ERK1/2 and STAT3 in liver lysates of AF6 LKO mice or Ad-AF6–infected mice, and our results demonstrated that AF6 has no effect on ERK2 or STAT3 activation in the liver (Supplementary Fig. 13). Taken together, our observations suggest that AF6 controls hepatic glucose homeostasis and insulin sensitivity by modulating the insulin pathway in an SHP2-dependent manner. Interestingly, the interaction between AF6 and SHP2 was increased in insulin-stimulated primary hepatocytes. This raises the possibility that insulin induces the recruitment of an AF6-SHP2 complex and reduces IRS1/AKT signaling, forming a negative feedback loop.

We believe that increased IRS1/AKT signaling is likely the primary cause of the enhanced glucose tolerance and insulin sensitivity in AF6 LKO mice, although we cannot entirely rule out other possibilities that may contribute to the phenotype of these mice. Kubota et al. (44) and Dong et al. (45) reported that IRS1 and IRS2 play overlapping roles in insulin action using conditional hepatic KOs of IRS1 and IRS2. Our data indicate that insulin-stimulated tyrosyl phosphorylation of IRS2 is also increased by hepatic AF6 depletion, whereas tyrosyl phosphorylation of IRS1 may be increased to a greater extent.

The regulation of cell polarity and metabolism are two biologically essential processes that have to be strictly controlled. Recent reports have implicated the emerging role of cell polarity proteins in the regulation of metabolism (6–12). With the use of RNA sequencing, significant progress has been made in understanding the transcript expression of a set of polarity genes in meta-inflammation (C.D., X.W., unpublished observations). On the basis of these findings, we found that high expression of the polarity protein AF6 can directly induce hyperglycemia and insulin resistance in vitro and in vivo and that knockdown of AF6 helps to alleviate glucose metabolism disorders in diabetic mice. To investigate whether the effects of AF6 on glucose metabolism link its role in polarity, we performed

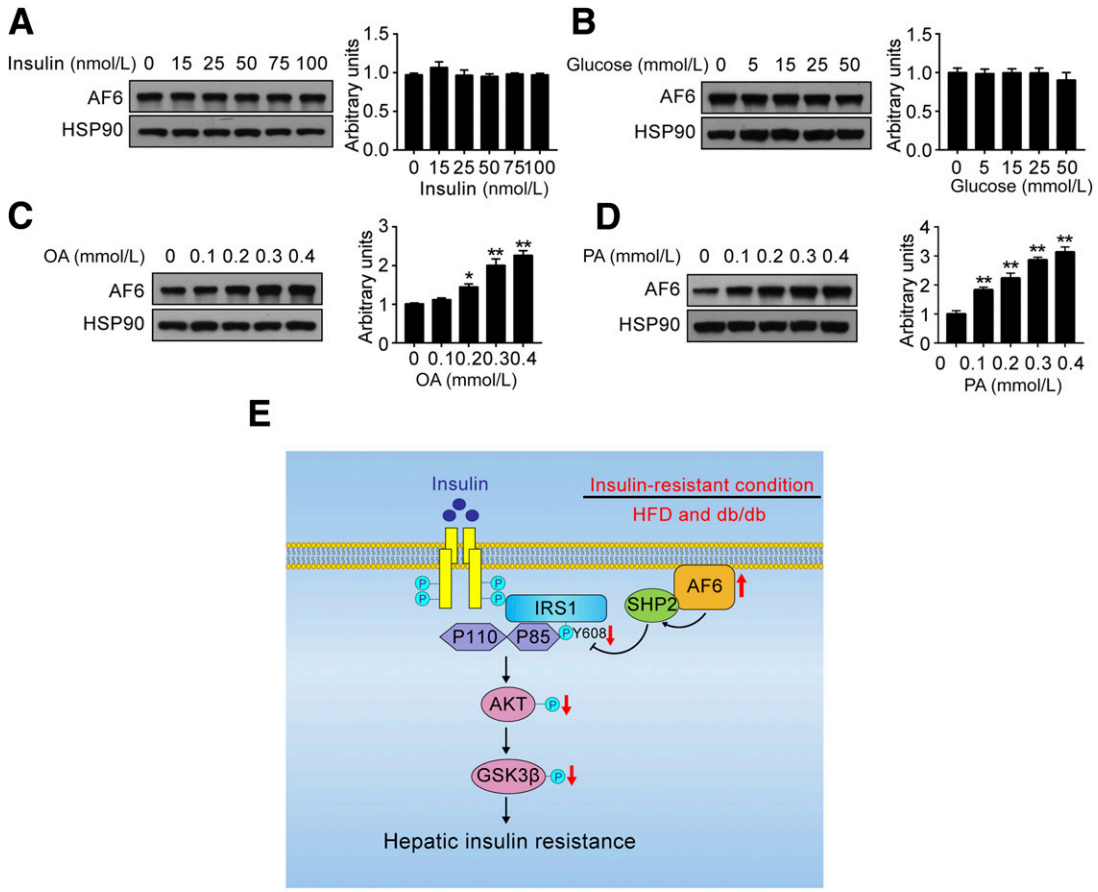

Figure 8—AF6 expression level was influenced by nutrition in hepatocytes. *A–D*: Mouse primary hepatocytes fasted overnight were treated with various concentrations of insulin (*A*), glucose (*B*), OA (*C*), or PA (*D*) for 6 h to examine the protein levels of AF6 by Western blot and quantified relative to HSP90. *E*: Working model of the role of hepatic AF6 in insulin sensitivity regulation. Statistical analysis was performed using one-way ANOVA. Data were obtained with at least three independent experiments and are mean ± SEM. $^{*}P < 0.05$, $^{**}P < 0.01$ vs. untreated primary hepatocytes.

immunofluorescence analysis for E-cadherin and ZO-1, two key proteins responsible for maintaining apicobasal cell adhesion and polarity, in the livers of AF6 LKO and AF6 fl/fl mice under chow- and HFD-fed states (Supplementary Fig. 14). We found that depletion of AF6 itself could not significantly change the expression or localization of these two polarity markers. The well-organized hepatic structure was significantly disrupted in HFD-fed mouse liver. Importantly, AF6 deletion did not rescue the disrupted apicobasal polarity observed in the livers of HFD-fed mice. Given that AF6 deletion significantly alleviates hyperglycemia and insulin resistance in HFD-induced diabetic mice (Fig. 7*A–E*), we conclude that the action of AF6 on glucose metabolism and hepatic insulin signaling is mediated through an SHP2-dependent IRS1/AKT pathway, not through the role of AF6 in cell polarity.

In conclusion, the current study reports a novel role for AF6 in insulin resistance and diabetes. Using in vivo and in vitro experiments, we demonstrated that abnormal AF6 expression can directly impair insulin signaling and induce insulin resistance by binding to SHP2 and upregulating SHP2's tyrosine phosphatase activity (Fig. 8*E*). These findings will provide new insights into the diverse functions of cell polarity proteins and further suggest that AF6 could be targeted as a therapeutic avenue for the treatment of diabetes, potentially facilitating improved insulin sensitivity and glucose tolerance.

Acknowledgments. The authors thank Dr. Jiali Deng, Dr. Yajie Guo, and Dr. Yi Luan (CAS Key Laboratory of Nutrition, Metabolism and Food Safety) for technical assistance; Dr. Yingying Le (CAS Key Laboratory of Nutrition, Metabolism and Food Safety) for helpful discussion; and Dr. Yong Liu (Hubei Key Laboratory of Cell Homeostasis, College of Life Sciences, Institute for Advanced Studies, Wuhan University, Wuhan, China) for providing the HFD-fed mouse liver samples.

Funding. This work was supported by grants from the National Key R&D Program of China (2017YFC1600100), the Strategic Priority Research Program of the Chinese Academy of Sciences (XDA12010100), and the National Natural Science Foundation of China (81672965, 81872369).

Duality of Interest. No potential conflicts of interest relevant to this article were reported.

Author Contributions. C.D., X.W., Y.W., and S.Z. researched data. C.D. and L.Z. designed the research and wrote, reviewed, and edited the manuscript. Y.X. and S.Z. contributed to the writing of the manuscript. M.Q. and

W.J. contributed to the discussion. L.Z. is the guarantor of this work and, as such, had full access to all the data in the study and takes responsibility for the integrity of the data and the accuracy of the data analysis.

References

1. Haffner S, Taegtmeyer H. Epidemic obesity and the metabolic syndrome. Circulation 2003;108:1541–1545
2. Stumvoll M, Goldstein BJ, van Haeften TW. Type 2 diabetes: principles of pathogenesis and therapy. Lancet 2005;365:1333–1346
3. Johnson AM, Olefsky JM. The origins and drivers of insulin resistance. Cell 2013;152:673–684
4. Samuel VT, Shulman GI. Mechanisms for insulin resistance: common threads and missing links. Cell 2012;148:852–871
5. Postic C, Dentin R, Girard J. Role of the liver in the control of carbohydrate and lipid homeostasis. Diabetes Metab 2004;30:398–408
6. Shaw RJ, Lamia KA, Vasquez D, et al. The kinase LKB1 mediates glucose homeostasis in liver and therapeutic effects of metformin. Science 2005;310:1642–1646
7. Sakamoto K, McCarthy A, Smith D, et al. Deficiency of LKB1 in skeletal muscle prevents AMPK activation and glucose uptake during contraction. EMBO J 2005;24:1810–1820
8. Koh HJ, Arnolds DE, Fujii N, et al. Skeletal muscle-selective knockout of LKB1 increases insulin sensitivity, improves glucose homeostasis, and decreases TRB3. Mol Cell Biol 2006;26:8217–8227
9. Granot Z, Swisa A, Magenheim J, et al. LKB1 regulates pancreatic beta cell size, polarity, and function. Cell Metab 2009;10:296–308
10. Fu A, Ng AC, Depatie C, et al. Loss of Lkb1 in adult beta cells increases beta cell mass and enhances glucose tolerance in mice. Cell Metab 2009;10:285–295
11. Lennerz JK, Hurov JB, White LS, et al. Loss of Par-1a/MARK3/C-TAK1 kinase leads to reduced adiposity, resistance to hepatic steatosis, and defective gluconeogenesis. Mol Cell Biol 2010;30:5043–5056
12. Hurov JB, Huang M, White LS, et al. Loss of the Par-1b/MARK2 polarity kinase leads to increased metabolic rate, decreased adiposity, and insulin hypersensitivity in vivo. Proc Natl Acad Sci U S A 2007;104:5680–5685
13. Mandai K, Nakanishi H, Satoh A, et al. Afadin: a novel actin filament-binding protein with one PDZ domain localized at cadherin-based cell-to-cell adherens junction. J Cell Biol 1997;139:517–528
14. Ponting CP. AF-6/cno: neither a kinesin nor a myosin, but a bit of both. Trends Biochem Sci 1995;20:265–266
15. Ikeda W, Nakanishi H, Miyoshi J, et al. Afadin: a key molecule essential for structural organization of cell-cell junctions of polarized epithelia during embryogenesis. J Cell Biol 1999;146:1117–1132
16. Radziwill G, Weiss A, Heinrich J, et al. Regulation of c-Src by binding to the PDZ domain of AF-6. EMBO J 2007;26:2633–2644
17. Takai Y, Ikeda W, Ogita H, Rikitake Y. The immunoglobulin-like cell adhesion molecule nectin and its associated protein afadin. Annu Rev Cell Dev Biol 2008;24:309–342
18. Radziwill G, Erdmann RA, Margelisch U, Moelling K. The Bcr kinase downregulates Ras signaling by phosphorylating AF-6 and binding to its PDZ domain. Mol Cell Biol 2003;23:4663–4672
19. Mandai K, Rikitake Y, Shimono Y, Takai Y. Afadin/AF-6 and canoe: roles in cell adhesion and beyond. Prog Mol Biol Transl Sci 2013;116:433–454
20. Tanaka-Okamoto M, Hori K, Ishizaki H, et al. Involvement of afadin in barrier function and homeostasis of mouse intestinal epithelia. J Cell Sci 2011;124:2231–2240
21. Chatterjee S, Seifried L, Feigin ME, et al. Dysregulation of cell polarity proteins synergize with oncogenes or the microenvironment to induce invasive behavior in epithelial cells. PLoS One 2012;7:e34343
22. Rives-Quinto N, Franco M, de Torres-Jurado A, Carmena A. Synergism between *canoe* and *scribble* mutations causes tumor-like overgrowth via Ras activation in neural stem cells and epithelia. Development 2017;144:2570–2583
23. Sullivan BP, Kopec AK, Joshi N, et al. Hepatocyte tissue factor activates the coagulation cascade in mice. Blood 2013;121:1868–1874
24. Xu Y, Chang R, Peng Z, et al. Loss of polarity protein AF6 promotes pancreatic cancer metastasis by inducing Snail expression. Nat Commun 2015;6:7184
25. Worby CA, Gentry MS, Dixon JE. Malin decreases glycogen accumulation by promoting the degradation of protein targeting to glycogen (PTG). J Biol Chem 2008;283:4069–4076
26. Lo S, Russell JC, Taylor AW. Determination of glycogen in small tissue samples. J Appl Physiol 1970;28:234–236
27. Roach PJ, Depaoli-Roach AA, Hurley TD, Tagliabracci VS. Glycogen and its metabolism: some new developments and old themes. Biochem J 2012;441:763–787
28. Girard J, Ferré P, Foufelle F. Mechanisms by which carbohydrates regulate expression of genes for glycolytic and lipogenic enzymes. Annu Rev Nutr 1997;17:325–352
29. Radziuk J, Pye S. Hepatic glucose uptake, gluconeogenesis and the regulation of glycogen synthesis. Diabetes Metab Res Rev 2001;17:250–272
30. Nakata S, Fujita N, Kitagawa Y, Okamoto R, Ogita H, Takai Y. Regulation of platelet-derived growth factor receptor activation by afadin through SHP-2: implications for cellular morphology. J Biol Chem 2007;282:37815–37825
31. Matsuo K, Delibegovic M, Matsuo I, et al. Altered glucose homeostasis in mice with liver-specific deletion of Src homology phosphatase 2. J Biol Chem 2010;285:39750–39758
32. Toyoshima D, Mandai K, Maruo T, et al. Afadin regulates puncta adherentia junction formation and presynaptic differentiation in hippocampal neurons. PLoS One 2014;9:e89763
33. Haskin J, Szargel R, Shani V, et al. AF-6 is a positive modulator of the PINK1/parkin pathway and is deficient in Parkinson's disease. Hum Mol Genet 2013;22:2083–2096
34. Basil AH, Sim JPL, Lim GGY, et al. AF-6 protects against dopaminergic dysfunction and mitochondrial abnormalities in *Drosophila* models of Parkinson's disease. Front Cell Neurosci 2017;11:241
35. Zankov DP, Sato A, Shimizu A, Ogita H. Differential effects of myocardial afadin on pressure overload-induced compensated cardiac hypertrophy. Circ J 2017;81:1862–1870
36. Fournier G, Cabaud O, Josselin E, et al. Loss of AF6/afadin, a marker of poor outcome in breast cancer, induces cell migration, invasiveness and tumor growth. Oncogene 2011;30:3862–3874
37. Yamamoto T, Mori T, Sawada M, et al. Loss of AF-6/afadin induces cell invasion, suppresses the formation of glandular structures and might be a predictive marker of resistance to chemotherapy in endometrial cancer. BMC Cancer 2015;15:275
38. Hwang JH, Perseghin G, Rothman DL, et al. Impaired net hepatic glycogen synthesis in insulin-dependent diabetic subjects during mixed meal ingestion. A ^{13}C nuclear magnetic resonance spectroscopy study. J Clin Invest 1995;95:783–787
39. Taniguchi CM, Emanuelli B, Kahn CR. Critical nodes in signalling pathways: insights into insulin action. Nat Rev Mol Cell Biol 2006;7:85–96
40. Myers MG Jr., Mendez R, Shi P, Pierce JH, Rhoads R, White MF. The COOH-terminal tyrosine phosphorylation sites on IRS-1 bind SHP-2 and negatively regulate insulin signaling. J Biol Chem 1998;273:26908–26914
41. Goldstein BJ, Bittner-Kowalczyk A, White MF, Harbeck M. Tyrosine dephosphorylation and deactivation of insulin receptor substrate-1 by protein-tyrosine phosphatase 1B. Possible facilitation by the formation of a ternary complex with the Grb2 adaptor protein. J Biol Chem 2000;275:4283–4289
42. Bard-Chapeau EA, Yuan J, Droin N, et al. Concerted functions of Gab1 and Shp2 in liver regeneration and hepatoprotection. Mol Cell Biol 2006;26:4664–4674
43. Bard-Chapeau EA, Li S, Ding J, et al. Ptpn11/Shp2 acts as a tumor suppressor in hepatocellular carcinogenesis. Cancer Cell 2011;19:629–639

44. Kubota N, Kubota T, Itoh S, et al. Dynamic functional relay between insulin receptor substrate 1 and 2 in hepatic insulin signaling during fasting and feeding. Cell Metab 2008;8:49–64

45. Dong XC, Copps KD, Guo S, et al. Inactivation of hepatic Foxo1 by insulin signaling is required for adaptive nutrient homeostasis and endocrine growth regulation. Cell Metab 2008;8:65–76